JOURNAL OF SPACECRAFT AND ROCKETS
Vol. 38, No. 1, January–February 2001

Three-Dimensional Numerical Simulation of Field-Emission-Electric-Propulsion Backflow Contamination

M. Tajmar*
Austrian Research Centers Seibersdorf, A-2444 Seibersdorf, Austria
and
J. Wang†
Jet Propulsion Laboratory, California Institute of Technology, Pasadena, California 91109

A three-dimensional full particle particle-in-cell with Monte Carlo collision simulation model is developed to study charge-exchange ion backflow from a field-emission-electric-propulsion thruster using liquid cesium as a propellant. Contamination from backflow of low-energy charge-exchange ions generated in the plume is an important spacecraft integration issue. Simulations show that the backflow ion current is on the order of 0.01% of the total emitting current under typical thruster operating conditions. Nearly all charge-exchange ions are collected by the accelerator electrode close to the emitter. Operating a field emission thruster at lower neutral flux, lower emitter current, or higher emitter potentials helps to reduce the backflow current and possible spacecraft contamination. The operation of a neutralizer does not have a significant effect on the backflow current under typical space plasma environments. A semi-analytical expression is also derived for quick estimations of the field emission thruster backflow current.

Nomenclature

A_{acc}	=	accelerator area, m^2
A_e, A_i, A_n	=	exit area of the electron, ion, and neutral beam, m^2
a	=	emitter–accelerator distance, m
b	=	half of accelerator aperature, m
C	=	proportional constant, $sm^{-2}C^{-1}$
c	=	neutralizer cathode accelerator distance, m
d	=	emitter slit depth, m
E	=	electric field, Vm^{-1}
e	=	electric charge, 1.602×10^{-19} C
I_B, $I_{B,\text{loss}}$, I_i	=	backflow, charge-exchange current lost in domain, and ion current, A
k	=	Boltzmann constant, 1.381×10^{-23} JK^{-1}
l	=	emitter slit length, m
m_e, m_i, m_n	=	electron, ion, and neutral mass, kg
N_{CEX}	=	charge-exchange number density, m^{-3}
n_i, n_n	=	ion, and neutral number density, m^{-3}
r	=	radius from emitter slit, m
r_c	=	neutralizer cathode radius, m
T_n	=	neutral temperature, K
U_{acc}	=	accelerator potential, V
U_E	=	emitter potential, V
U_{exit}	=	potential in the exit area of the slit emitter, V
v_e, v_{CEX}, v_i, v_n	=	electron, charge-exchange ion, ion, and neutral velocity, ms^{-1}
w	=	emitter slit width, m
α	=	geometric divergence angle, deg
Γ	=	thermal flux, $s^{-1}m^{-2}$
γ	=	neutral transmission factor, %
ε_0	=	electric constant, 8.854×10^{-12} Fm^{-1}
ϑ_i	=	divergence angle perpendicular to the slit direction, deg
λ_D	=	debye length, m
ν_{CEX}	=	charge-exchange collision frequency, s^{-1}
ρ	=	charge density, Cm^{-3}
σ_{CEX}	=	charge-exchange cross section, m^{-2}
φ_i	=	divergence angle along the slit direction, deg
ϕ	=	potential, V

Received 13 December 1999; revision received 25 September 2000; accepted for publication 25 September 2000.

*Staff Member, Space Propulsion Group; martin.tajmar@arcs.ac.at.
†Senior Member of Engineering Staff, Advanced Propulsion Technology Group, MS125-224, 4800 Oak Grove Drive; joseph.j.wang@jpl.nasa.gov. Member AIAA.

Introduction

AN advanced electrostatic propulsion concept that can provide high precision thrust at high specific impulse[1] is field-emission-electric-propulsion (FEEP). A FEEP device using liquid cesium as a propellant consists of a positive emitter slit and a negative accelerator electrode (Fig. 1), where a potential difference on the order of 10 kV is applied to generate a strong electric field at the tip of the liquid metal surface (Taylor cones) of the emitter. This electric field extracts cesium ions from the tip of the emitter and accelerates them through the accelerator. FEEP's performance characteristics make it ideal for missions that require precision spacecraft control over a multiyear lifetime, such as interferometry missions involving multiple spacecrafts flying in formation.

Whereas a FEEP thruster offers a unique propulsion capability, it also raises concerns over potential contaminations because a propellant of liquid metal can be a harmful contamination source. In addition to the propellant ions, a FEEP thruster also emits a neutral flux. The neutral flux consists of neutral atoms evaporized from the liquid-metal surface inside the emitter slit due to its temperature, as well as neutral microdroplets (with diameters smaller then 2×10^{-9} m) and neutral atoms extracted during field emission.[2] Charge-exchange collisions will occur between the beam ions and the atomic neutral components, producing low energy charge-exchange ions that can backflow to the spacecraft.

Charge-exchange ion backflow from conventional ion thrusters has been a subject of extensive research (for example, Refs. 3–5). All ion thrusters now use noble gas, such as xenon, as a propellant to minimize the contamination potential. Because FEEP is a relatively new technology, there have been few experimental or theoretical studies to characterize FEEP's plume and the induced backflow contamination other than a mass spectroscopic measurement of FEEP plume composition[2] and recent ion current profile measurements.[6]

The objective of this paper is to develop a three-dimensional numerical model for FEEP charge-exchange ion backflow assessment. In a previous study, Tajmar and Wang have developed a three-dimensional numerical model for FEEP neutralization[7] where a full particle particle-in-cell (PIC) model is used to simulate FEEP ions and neutralizer electrons under different ambient plasma conditions. That three-dimensional simulation code was tested against the ion density measurements obtained for a FEEP

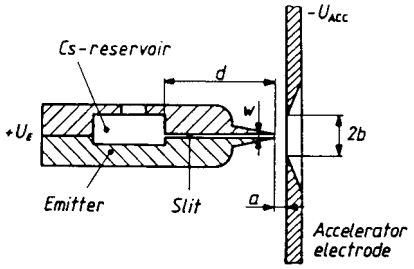

Fig. 1 Sectional view of the emitter–accelerator electrode configuration.[1]

emitter at Centrospazio,[8] and the results show a good agreement with measurements.[9] Here, the model developed by Tajmar and Wang[7] is extended to included charge-exchange ion interactions.

The numerical model presented in this paper is based on a three-dimensional, full-particle PIC with Monte Carlo collisions between the ion and the neutral particles. In this paper, we study the basic characteristics of the propellant ions and neutrals emitted from a FEEP thruster and the charge exchange ions generated within the plume. We study the effects from ambient plasmas and neutralizer electrons on the potential field and on the charge-exchange ions. We investigate the effects of FEEP operating conditions on backflow contaminations. The simulation results, combined with mass spectroscopic measurements, are used to predict three-dimensional spatial distributions of the backflow ions on the spacecraft surface and suggest FEEP design considerations to reduce contaminations. We also derive an analytical expression that allows one to scale the results of contamination predictions for operating conditions not considered in this paper.

Formulation

The numerical model is an extension from the one by Tajmar and Wang to study FEEP neutralization.[7] The FEEP thruster considered here (Fig. 1) is similar to that tested at Centrospazio[8] and other FEEP emitter experiments.[1] Typical basic parameters for this thruster are summarized in Table 1. The neutralizer considered is a thermionic cathode, which consists of a hot filament underneath a small accelerator cathode. Basic parameters for the neutralizer are summarized in Table 2.

In a FEEP emitter, ion emission originates from the emitter surface located at a distance a (emitter–accelerator distance) behind the accelerator electrode (Fig. 1). Typically, the accelerator electrode of the FEEP emitter is placed on the spacecraft surface. The emitter electrode has a positive potential U_E with respect to the spacecraft potential, and the accelerator electrode has a negative potential U_{acc} with respect to the spacecraft potential. The geometry of the electrodes creates a focused ion beam, which is accelerated through the accelerator. The velocity of the beam ions at the FEEP's exit, v_i, is given by

$$v_i = \sqrt{[2 \cdot (U_E - U_{\text{exit}}) \cdot e]/m_i} \tag{1}$$

Note that U_{exit} is a function of U_E, U_{acc}, and the beam ion density and needs to be determined self-consistently by taking the space charge into account. At a FEEP's exit, to a good approximation, the propellant ions are focused into a Gaussian distribution[6] limited to the divergence angles ϑ_i perpendicular to the slit direction and φ_i along the slit direction due to FEEP's geometry. If the ions were perfectly neutralized and there were no space charge effects, they would form a beam according to this divergence angle. Under this condition, the cross section of the ion beam near the FEEP exit would be

$$A_i = (l + 2a \cdot \tan\varphi_i) \cdot (w + 2a \cdot \tan\vartheta_i) \tag{2}$$

When the ion current I_i is used, the ion density n_i at the FEEP's exit can be expressed by

$$n_i = I_i/(e \cdot A_i \cdot v_i) \tag{3}$$

Table 1 FEEP emitter parameters

Parameter	FEEP emitter
Slit length l, cm	1.5
Slit width w, μm	1.5
Accelerator length, cm	4
Accelerator width, cm	1
Emitter–accelerator distance a, mm	0.6
Accelerator aperature b, mm	2
Ion divergence perpendicular to slit ϑ_i, deg	30
Ion divergence in slit direction φ_i, deg	15
Neutral temperature T_n, K	305

Table 2 Neutralizer parameters

Parameter	Thermionic neutralizer
Inner cathode diameter, mm	3
Cathode–anode distance, mm	0.3
Electron divergence in all directions, deg	30

In a thermionic cathode neutralizer, electron emission can be considered to originate from a point source in the middle of the accelerator cathode where the electrons are then accelerated by the anode potential U_A. The exit electron velocity v_e is a combination of the thermal velocity of the hot-filament-generated Maxwellian velocity distribution with the cathode at temperature T and the acceleration due to the anode:

$$v_e = \sqrt{8kT/m_e\pi} + \sqrt{2eU_A/m_e} \tag{4}$$

In the absence of space charge effects, the spatial distribution of the emitted electrons at the exit can be modeled by a simple cosine distribution squeezed in all directions by a divergence angle β. For a given cathode radius r_c, the cross-sectional area of the electron beam at the neutralizer's exit, A_e, is given by

$$A_e = (r_c + c \cdot \tan\beta)^2 \cdot \pi \tag{5}$$

where c is the neutralizer cathode–accelerator distance. The electron density at the neutralizer's exit can be expressed similar to the ion density in Eq. (3).

The neutral flux emitted by the FEEP thruster consists of 1) thermal neutrals evaporized from the free liquid-metal surface (which has a temperature of about 300 K) inside the emitter slit and 2) neutrals extracted by field emission. The second component includes microdroplets with a diameter smaller than 2×10^{-9} m and atomic neutral particles. The presence of the neutral atoms is theoretically still unexplained. One hypothesis is that some microdroplets would dissociate under strong electric forces and become neutral atoms.[2,10] For the FEEP emitter considered here, the neutral atom flux has been measured to be approximately 1% of the beam ion flux and is about two orders of magnitude higher than that of the neutrals from thermal evaporation at a temperature of 300 K. Hence, for charge-exchange calculations, we shall consider only the neutral atom flux from field emission.

We assume that the field emitted neutrals follow a Maxwell–Boltzmann distribution with a mean thermal velocity v_n:

$$v_n = \sqrt{8kT_n/m_n\pi} \tag{6}$$

The propagation of the neutrals is not affected by the potentials but by the accelerator geometry, which can be approximated to a squeezed cosine distribution with a maximum divergence angle α both in the direction and perpendicular to the direction of the slit, which is the limit given by the geometry.[2] Hence, the cross section of the neutral beam would be

$$A_n = (l + 2a \cdot \tan\alpha) \cdot (w + 2a \cdot \tan\alpha) \tag{7}$$

The neutral mass emission rate $\mathrm{d}m_n/\mathrm{d}t$ was measured to be proportional to the ion current I_i during field emission.[2] Hence, the ion

density n_i and neutral density n_n are related to the total emission current:

$$n_i = \frac{I_i}{eA_i v_i} \cdot \frac{(100-\gamma)}{100}, \qquad n_n = \frac{I_i \cdot \gamma}{eA_n v_n} \tag{8}$$

where γ is the proportional constant between the beam ion and the neutral flux.

Resonant charge-exchange collisions will occur between the beam ions and the neutrals. The collision frequency ν_{CEX} and the ion production rate per volume dN_{CEX}/dt is given by

$$\nu_{CEX} = n_n v_i \sigma_{CEX}(v_i), \qquad \frac{dN_{CEX}}{dt} = n_i n_n v_i \sigma_{CEX}(v_i) \tag{9}$$

where $\sigma_{CEX}(v_i)$ is the velocity-dependent charge-exchange cross section in square meters (we neglect the thermal neutral velocity v_n because it is four magnitudes below the ion velocity v_i), which can be expressed by[11]

$$\sigma_{CEX}(v_i) = (k_1 \ln v_i + k_2)^2 \tag{10}$$

For cesium, the constants are $k_1 = -1.492 \times 10^{-10}$ s and $k_2 = 2.6997 \times 10^{-9}$ m. From Eqs. (8) and (9), we summarize the charge-exchange production rate as

$$\frac{dN_{CEX}}{dt} = \frac{I_i^2 \cdot \gamma \cdot (100-\gamma)}{e^2 \cdot A_i \cdot A_n \cdot v_n \cdot 100} \cdot \sigma_{CEX}(v_i) \tag{11}$$

To study charge-exchange ion interactions, a full particle, three-dimensional electrostatic PIC code[12] has been developed. In this code, all plasma particles (beam ions, neutralizer electrons, ambient ions, and ambient electrons) and neutral particles are treated as computational test particles. Part of the spacecraft is modeled as a box in the middle of the bottom area of the simulation domain.

Test particles representing the FEEP ions are injected into the simulation domain (Fig. 2) along the FEEP slit on the spacecraft surface with the velocity v_i [Eq. (1)] and with a spatial distribution given by Eq. (2). Test particles representing the neutralizer electrons are injected into the simulation domain from the neutralizer exit with the velocity v_e [Eq. (4)], which follows the spatial distribution given by Eq. (5).

For simulations with an ambient plasma, test particles representing the ambient plasma are loaded uniformly into the domain with a Maxwellian velocity distribution at the start of the simulation. All domain boundaries except the spacecraft box are considered to be open boundaries. At the open boundaries, ambient plasma particles can flow into the simulation domain with a thermal flux

$$\Gamma = (n/4)\sqrt{8kT/m\pi} \tag{12}$$

A Neumann boundary condition for Poisson's equation is applied on all open boundaries, while the potentials at the surfaces of the spacecraft box, the emitter, accelerator, and neutralizer are specified. The trajectories of each plasma particle, the space charge, and the self-consistent electric field are obtained from Newton's second law and Poisson's equation, respectively:

$$F = m\frac{dv}{dt} = E \cdot q \tag{13}$$

$$-\nabla^2 \phi = \frac{\rho}{\varepsilon_0} \tag{14}$$

The neutral particles undergo a free molecular flow following the initial neutral beam distribution given by Eq. (7).

A Monte Carlo collision scheme is used to model charge-exchange collisions. The probability P for the collision between an ion and a neutral beam particle is calculated for every ion particle using the following equation[13]:

$$P = 1 - \exp[-v_{relative} \cdot \sigma_{CEX} \cdot n_n(x, y, z) \cdot dt] \tag{15}$$

where $v_{relative}$ is the velocity difference between the ion and the neutral particle and dt is the time step used in the simulation. We can approximate $v_{relative} = v_i$ because the neutral velocity is three orders of magnitude smaller than the ion velocity. The probability is multiplied by the test particle ratio between beam and charge-exchange ions. If P is greater than a random number R_n between 0 and 1 ($P > R_n$), a collision occurred and a charge-exchange test particle is created at that position. This can be done because the charge-exchange ion density is order of magnitudes below the ion and neutral density and, therefore, does not affect them.

The number of ions emitted from the FEEP emitter varied from case to case, but the number of particles per cell was always larger than 100 to minimize the effects of numerical noise. Numerical tests were also performed to ensure that the number of particles we used is sufficient so that it does not affect the steady-state situation. The time step for the ions and electrons was based on the electron plasma frequency. Because the calculation of the neutral particle trajectories is independent from that of the plasma particles, we choose a larger time step for the neutral. The time step for the neutrals is chosen so that they do not move more than one grid cell during each neutral particle time step. The simulation was performed until a steady state was reached, that is, the number of particles in the simulation domain remained constant. In a typical case, the number of particles at equilibrium was 270,000 with 255,000 ions and 15,000 neutrals using a test particle weight of $6E4$, $1E2$, and $1.5E6$ for beam ions, charge-exchange ions, and neutrals, respectively. The time step was 1.8×10^{-8} s, and the number of time steps to reach equilibrium was 2000. In all cases the collision frequency is well above the electron plasma frequency required for this Monte Carlo method. A typical run takes about 3–4 days on a 400 MHz personal computer workstation.

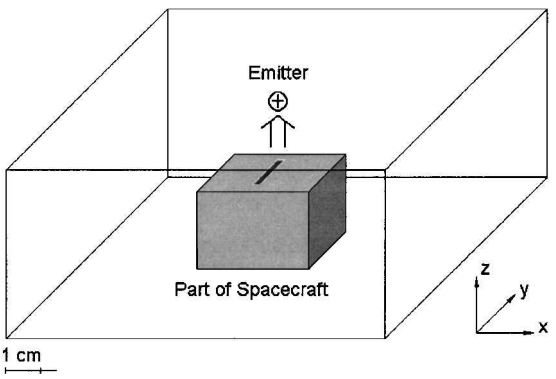

Fig. 2 Simulation domain.

Results and Discussion

Code Verification

As already mentioned, few experimental studies exist that characterize the FEEP plume. Recently Marcuccio et al.[6] published ion beam profile measurements using electrostatic stainless-steel wire probes biased at −200 V. We implemented such wire probes in our simulation by collecting the current at the probes distance using the wire's diameter of 0.8 mm, which we compared with the measurements. The FEEP emitter used in Ref. 6 is an old model with small manufacturing irregularities, which resulted in larger divergence angles perpendicular to the slit. However, all other parameters are comparable to the recent designs. The ESA emitter parameters are summarized in Table 3. Figures 3 and 4 compare the ion current obtained from simulation with the measurement reported in Ref. 6. In Fig. 3, the probe is positioned horizontally (perpendicular to the slit) at a distance of $R = 61$ mm from the thruster. In Fig. 4, the probe is positioned vertically (parallel to the slit) at a distance of $R = 92$ mm (at $Z = -41$ mm from the exit). In both cases, the agreement is very good, confirming our numerical approach.

Additionally, we have also compared the potential field calculated from this code with that obtained from a finite element model from Centrospazio,[14] and the results are shown in Fig. 5. In this case, the parameters for the FEEP thruster used here are $U_E = 8$ kV and $U_{acc} = -4$ kV. Again, the results are in good agreement.

Table 3 Code verification simulation parameters

Parameter	FEEP emitter
Slit length, l, cm	5
Slit width w, μm	1.2
Accelerator length, cm	4
Accelerator width, cm	1
Emitter–accelerator distance a, mm	0.5
Accelerator aperature b, mm	4
Ion divergence perpendicular to slit ϑ_i, deg	66
Ion divergence in slit direction φ_i, deg	20
Neutral temperature T_n, K	305
Ion current, mA	0.51
Emitter potential U_E, kV	8
Accelerator potential U_{acc}, kV	−2
Transmission factor γ, %	1

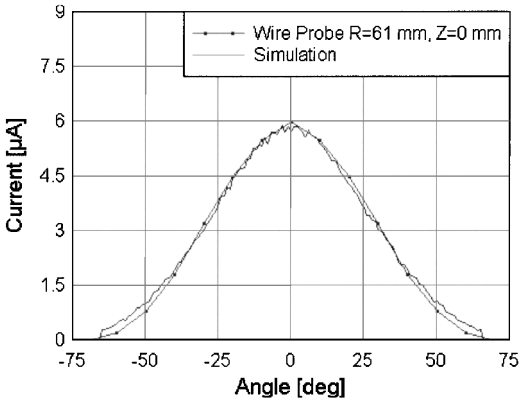

Fig. 3 Horizontal electrostatic wire probe comparison with data from Marcuccio et al.[6]

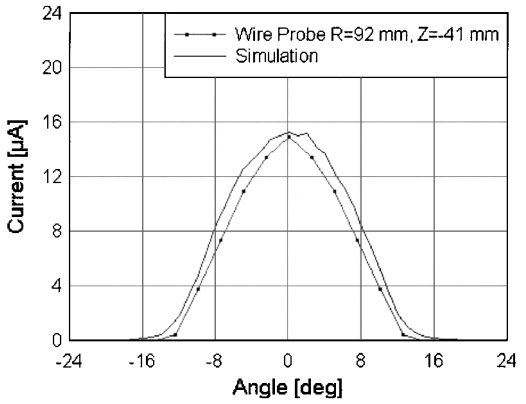

Fig. 4 Vertical electrostatic wire probe comparison with data from Marcuccio et al.[6]

Backflow Contamination Assessment

There are two major factors that will influence charge-exchange ion interactions. The first one is the potential distribution surrounding the plume and spacecraft, which determines the trajectory of a charge-exchange ion. The second one is the charge-exchange ion production rate, which is a function of the properties of the beam ions and neutrals. We are not able to simulate all possible scenarios due to computational constraints. Our previous study has shown that the potential field in the vicinity of FEEP can differ significantly under different neutralization environment.[7] Hence, we first simulate charge exchange ion backflow at the same operating condition but with different beam neutralization environments. We then simulate charge exchange ion backflow at different operating conditions under the same neutralization environment. The operating conditions are chosen to follow a measured FEEP current-voltage characteristic. Finally, we derive an analytical expression that can be used to estimate charge-exchange ion backflow under other circumstances based on simulation results and analytical calculations.

Charge-Exchange Ion Backflow Under Different Neutralization Environments

We consider the following three operation scenarios: case A, no neutralizer in vacuum environment; case B, neutralizer in vacuum environment located at 2.5 cm next to the FEEP emitter in the x direction; and case C, no neutralizer in laboratory plasma environment, as listed in Tables 4 and 5. In Ref. 7 the potential field under these three scenarios have been studied in detail in the absence of charge-exchange ions. In this work we concentrate on the region above the emitter slit and set the simulation domain to $0.05 \times 0.05 \times 0.05$ m and the number of grid cells to $20 \times 20 \times 20$. Extensive numerical tests have been performed to ensure that the grid resolution does not affect the steady-state solution.[7]

Figure 6 compares the potential along the middle of the slit emitter in the z direction for cases A, B, and C. These results are very similar to those presented in Ref. 7. The inclusion of charge-exchange ions does not change the potential field appreciably because space charge effects from charge-exchange ions are negligible compared to that of beam ions due to the low charge-exchange ion density. Figure 7 shows the potential distribution on an x–z plane across the beam.

As shown in Figs. 6 and 7, the potential near the slit is dominated by the exposed FEEP accelerator electrode. Because of the FEEP configuration, the beam ions cannot be neutralized effectively by electrons emitted from a neutralizer close by.[7] Hence, the potential field in case B does not differ significantly from that in case A. The ion beam can only be neutralized efficiently in case C because a laboratory environment provides ambient electrons with a density comparable to the FEEP ion density (in this case[7] $n_e = 2.4 \times 10^{14}$ m^{-3}). Space plasmas such as those in low Earth orbit ($n_e = 1 \times 10^{12}$ m^{-3}) contribute much less to neutralization having an effect, similar to the presented case B as shown in Ref. 7.

Table 4 summarizes the backflow charge-exchange ion current from simulations of the three cases. The backflow currents are calculated by integrating test particles deposited over the entire spacecraft

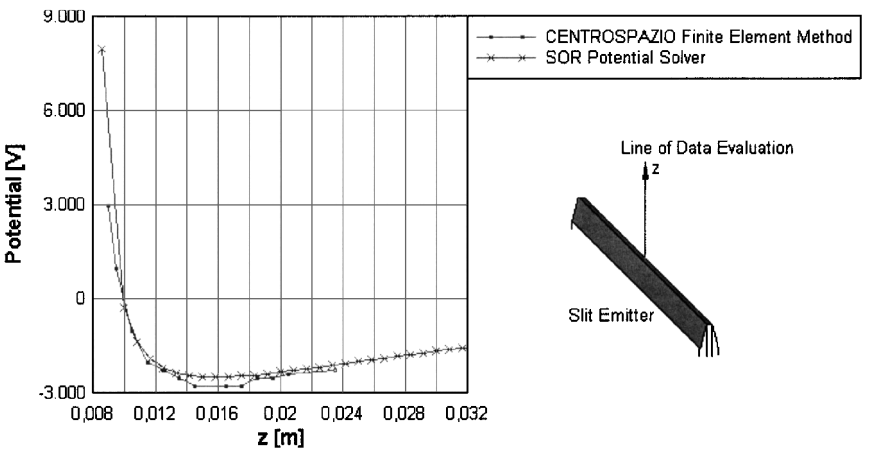

Fig. 5 Potential comparison with data from Andrenucci et al.[14]

Table 4 Simulation parameters and backflow currents in neutralized environment

Case	Neutralizer voltage, V	Neutralizer current, mA	Background plasma	Neutralizer	Backflow current I_B, mA
A	——	——	——	No	$4.01 \pm 0.01E-5$
B	100	1	——	Yes	$3.90 \pm 0.11E-5$
C	——	——	Laboratory	No	$2.90 \pm 0.04E-5$

Table 5 Simulation results

Case	Ion current I_i, mA	Emitter potential U_E, kV	Accelerator potential U_{acc}, kV	Transmission factor γ, %	Backflow current I_B, mA	CEX current loss $I_{B,loss}$, mA
1	1	3.5	−5	1	$4.01 \pm 0.01E-5$	$1.35 \pm 0.55E-8$
2	2	4.5	−5	1	$1.54 \pm 0.02E-4$	$2.71 \pm 0.56E-7$
3	3	5.5	−5	1	$3.44 \pm 0.04E-4$	$1.73 \pm 0.23E-6$
4	4	6.0	−5	1	$6.01 \pm 0.06E-4$	$4.49 \pm 0.56E-6$
5	5	6.5	−5	1	$9.30 \pm 0.02E-4$	$8.51 \pm 0.18E-6$
6A	2	3.5	−5	1	$1.59 \pm 0.02E-4$	$6.00 \pm 0.65E-7$
6B	3	3.5	−5	1	$3.56 \pm 0.04E-4$	$3.27 \pm 0.26E-6$
6C	4	3.5	−5	1	$6.24 \pm 0.05E-4$	$7.56 \pm 0.34E-6$
6D	5	3.5	−5	1	$9.81 \pm 0.07E-4$	$1.45 \pm 0.12E-5$
6E	6	3.5	−5	1	$1.40 \pm 0.01E-3$	$2.21 \pm 0.14E-5$
7A	1	4.5	−5	1	$3.95 \pm 0.04E-5$	$1.15 \pm 0.36E-8$
7B	1	5.5	−5	1	$3.89 \pm 0.03E-5$	$1.60 \pm 0.65E-8$
7C	1	6.5	−5	1	$3.83 \pm 0.03E-5$	$1.92 \pm 0.47E-8$
7D	1	7.5	−5	1	$3.79 \pm 0.02E-5$	$1.34 \pm 0.67E-8$
7E	1	8.5	−5	1	$3.73 \pm 0.05E-5$	$1.06 \pm 0.49E-8$
8A	1	3.5	−3	1	$4.09 \pm 0.02E-5$	$5.99 \pm 1.58E-8$
8B	1	3.5	−4	1	$4.07 \pm 0.03E-5$	$3.03 \pm 1.03E-8$
8C	1	3.5	−6	1	$3.96 \pm 0.04E-5$	$1.19 \pm 0.44E-8$
8D	1	3.5	−7	1	$3.92 \pm 0.05E-5$	$1.54 \pm 0.68E-8$
8E	1	3.5	−8	1	$3.90 \pm 0.04E-5$	$1.09 \pm 0.44E-8$
9A	1	3.5	−5	2	$7.98 \pm 0.07E-5$	$2.40 \pm 1.21E-8$
9B	1	3.5	−5	3	$1.20 \pm 0.01E-4$	$4.38 \pm 0.78E-8$
9C	1	3.5	−5	4	$1.60 \pm 0.01E-4$	$4.94 \pm 1.52E-8$
9D	1	3.5	−5	5	$2.00 \pm 0.01E-4$	$6.14 \pm 1.51E-8$
9E	1	3.5	−5	6	$2.40 \pm 0.01E-4$	$7.90 \pm 1.08E-8$

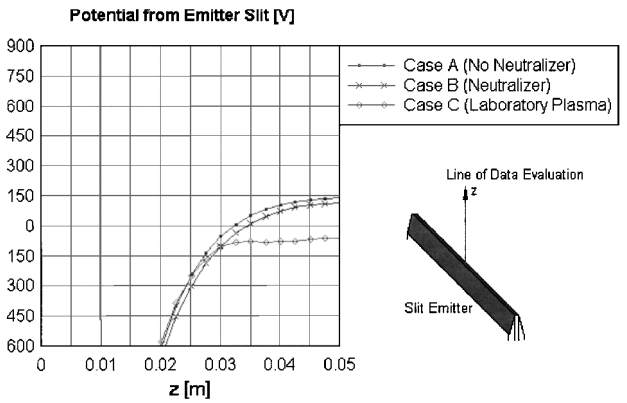

Fig. 6 Comparision of potential from middle of slit emitter between cases A, B, and C.

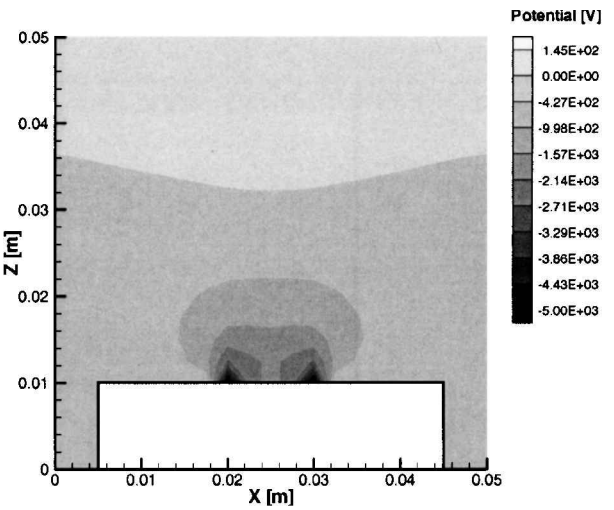

Fig. 7 Cases 1 and A, x–z potential plot at plane $y = 0.025$ m.

surface. The currents from case A (vacuum emission) and case B (operation of a neutralizer) are very similar (>97%); only case C (emission in laboratory plasma) shows a reduction of 28%.

The result of the backflow current is consistent with that for the potential field. Most charge-exchange collisions occur just above the slit, where both the ion and neutral density are at their maximum. Therefore, the region above the emitter slit will contribute most to the backflow current. Placing a neutralizer 3 cm above the spacecraft surface (case B) does not change the potential near the FEEP emitter's exit. Therefore, backflow currents in cases A and B are similar. On the other hand, the backflow current in case C differs from that in cases A and B due to the small debye length, $\lambda_{D,laboratory} \approx 1$ mm from the ambient plasma. The ambient plasma shields the negative accelerator electrode, and thus, fewer charge-exchange ions will be attracted by the exposed FEEP electrode. This reduces the total backflow current.

In the following sections, we shall concentrate on the in-space condition and neglect the background plasma. Furthermore, because including a neutralizer will only have a minimum effect on the potential field and charge-exchange ion backflow, we shall consider only the no-neutralizer scenario.

Charge-Exchange Ion Backflow Under Different Operating Conditions

We next consider charge-exchange ion backflow under different operating conditions. In all cases, the ion emission occurs in a vacuum environment without a neutralizer. Our first set of simulations (cases 1–5) concern operating conditions for the well measured FEEP current-voltage characteristic.[1] An increase of the ion current I_i along the current-voltage characteristic will result in an increase in

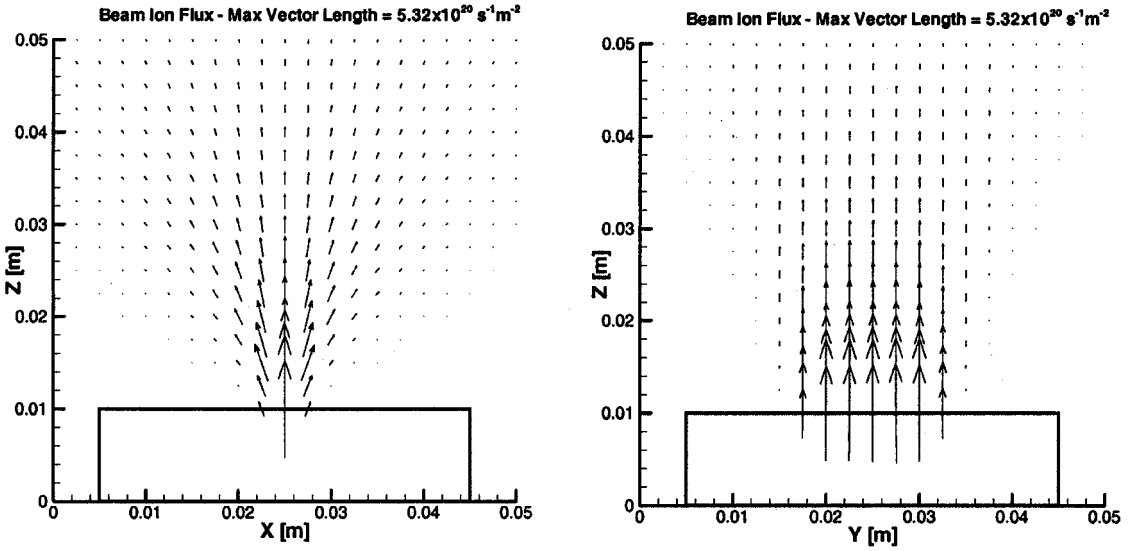

Fig. 8 Beam ion flux $n_i \cdot v_i$; plot x–z at plane $y = 0.025$ m and plot y–z at plane $x = 0.025$ m: case 5.

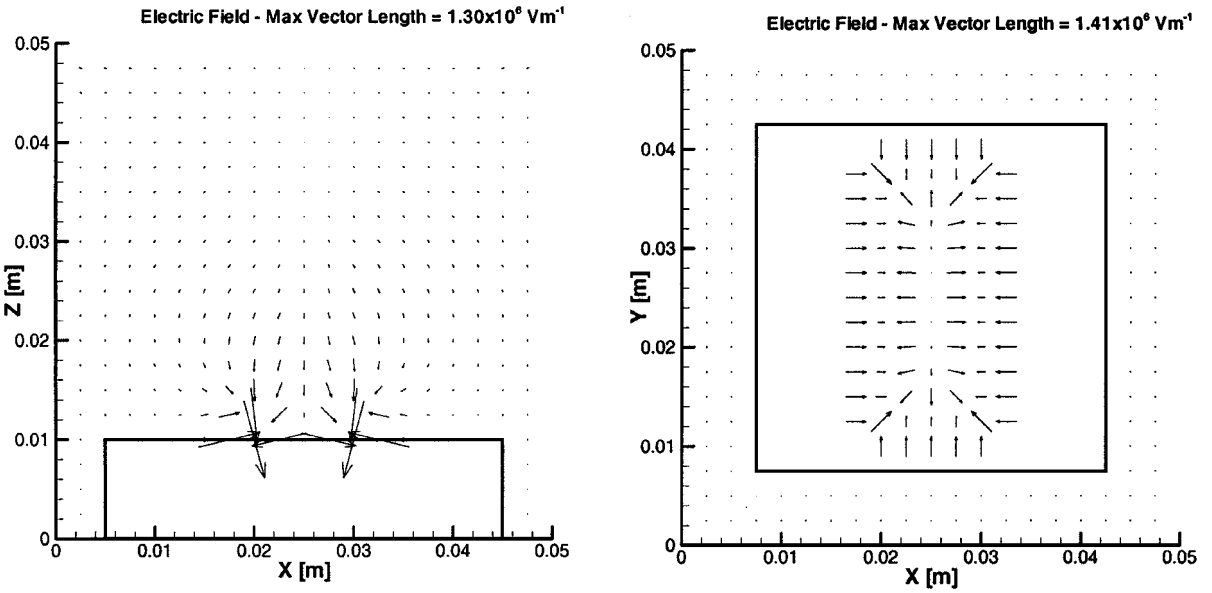

Plot of x–z at plane $y = 0.025$ m

Plot of x–y over spacecraft surface

Fig. 9 Electric field plots: case 5.

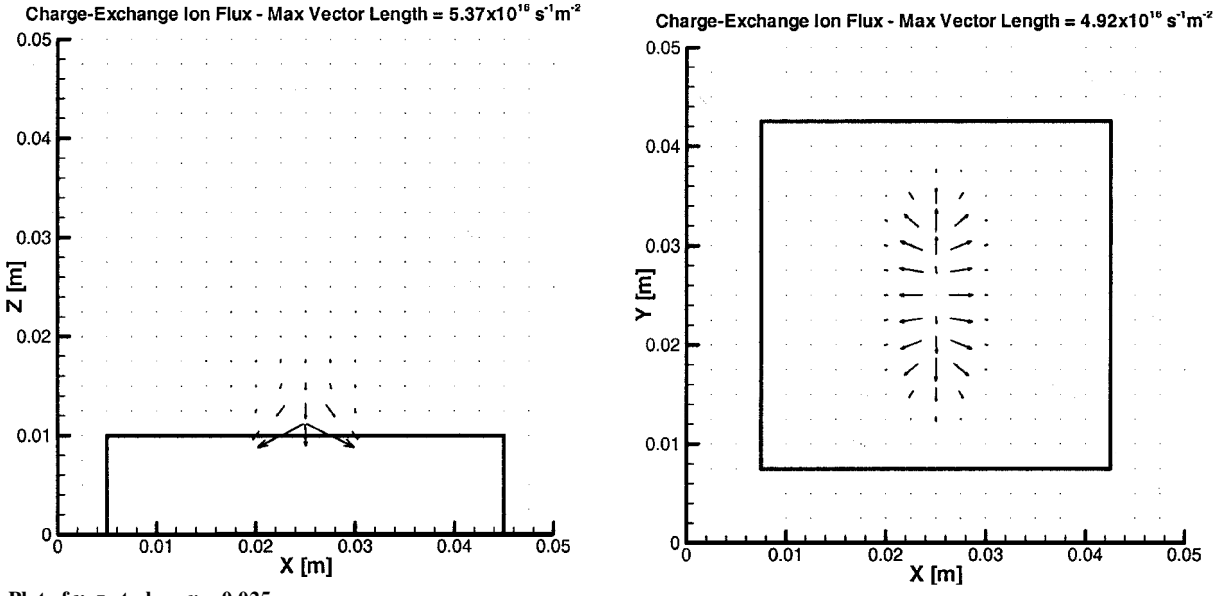

Plot of x–z at plane $y = 0.025$ m

Plot of x–y over spacecraft surface

Fig. 10 Charge-exchange ion flux $n_{\mathrm{CEX}} \cdot v_i$ plots: case 5.

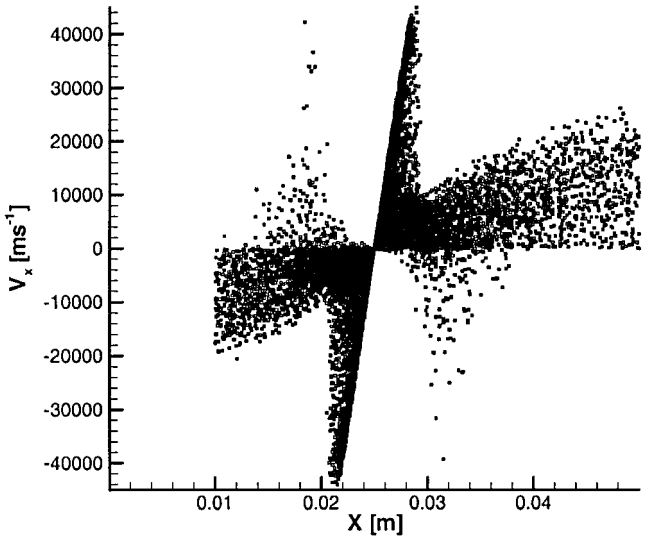

Phase plot of x–v_x

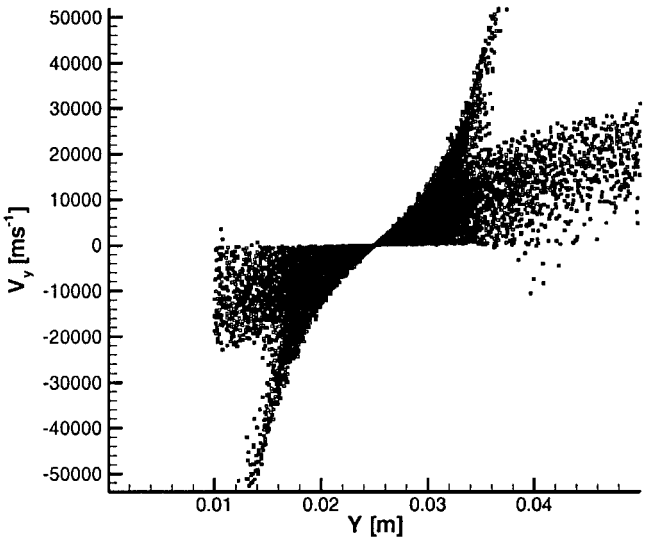

Phase plot of y–v_y

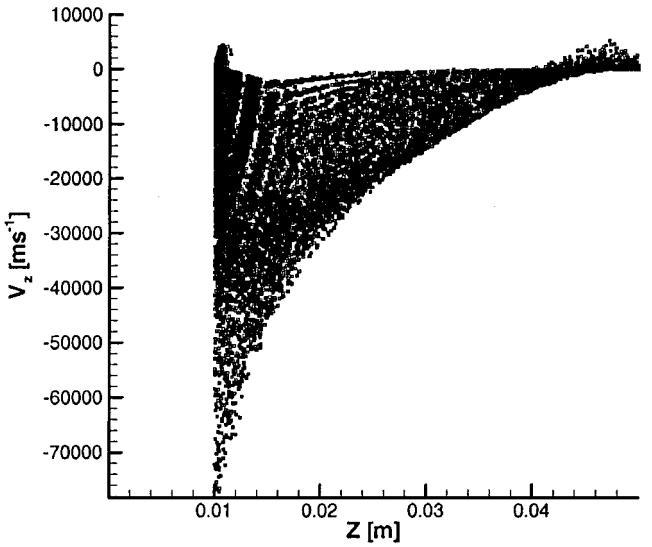

Phase plot of z–v_z

Fig. 11 Charge-exchange ion phase plots: case 5.

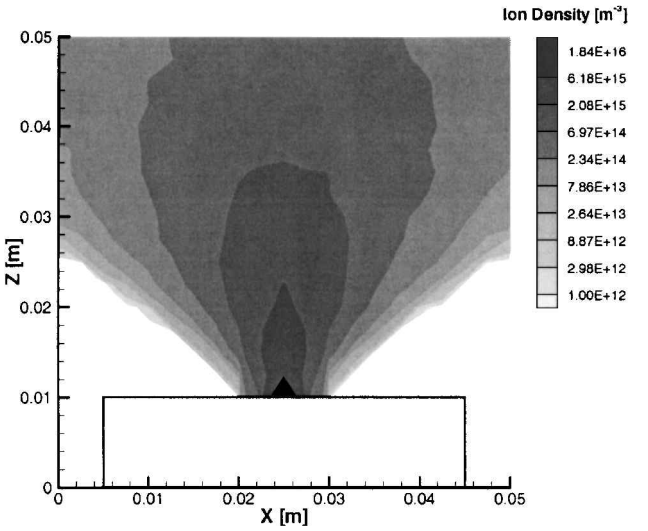

Beam ion density

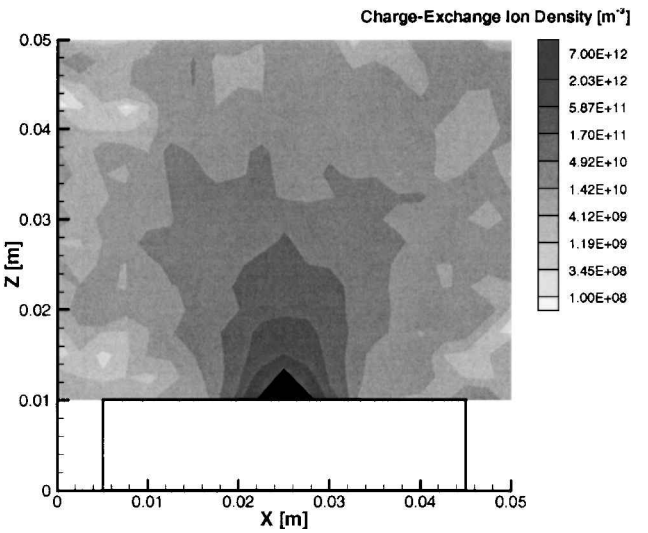

Charge-exchange ion density

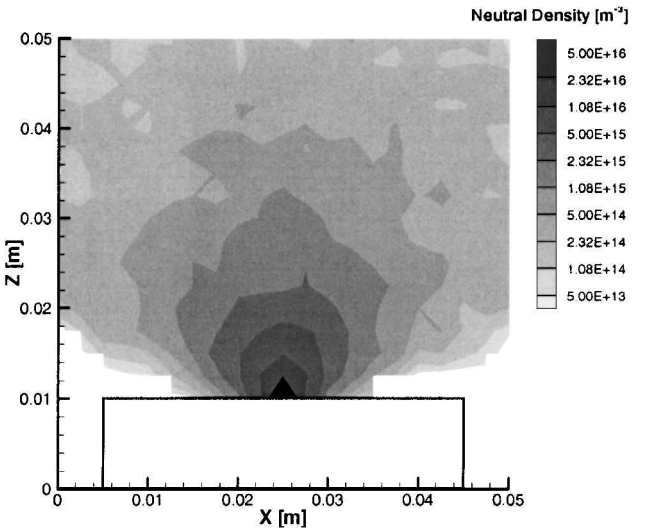

Neutral density

Fig. 12 The x–z density plots at plane y = 0.025 m: case 5.

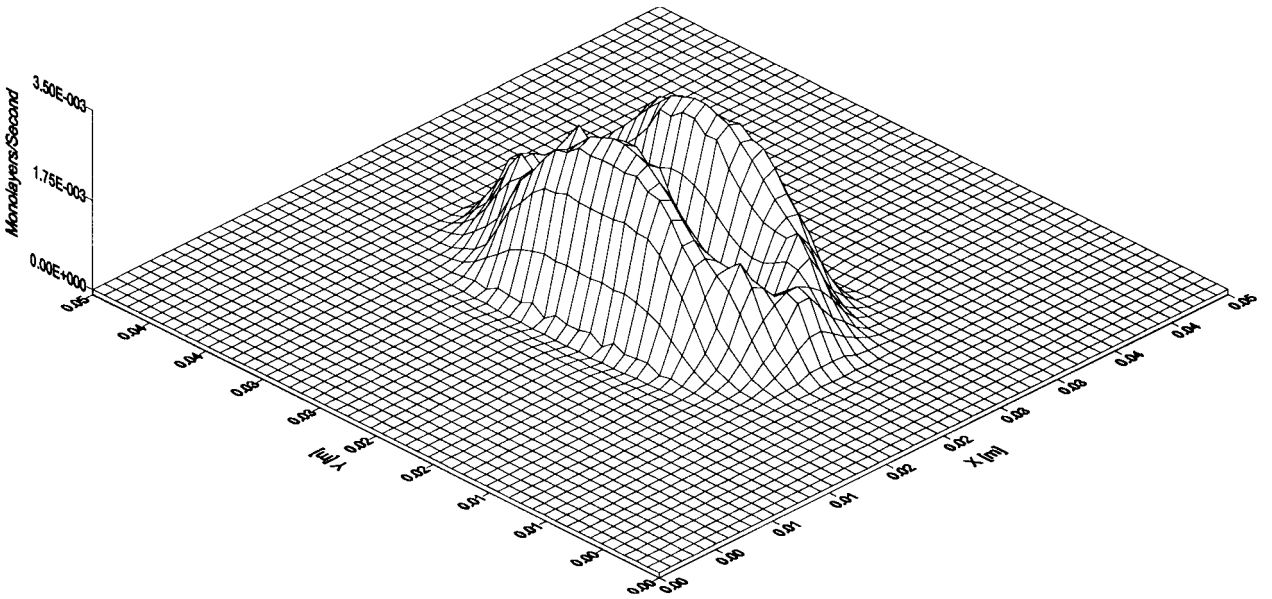

Fig. 13 Distribution of monolayers/s on the spacecraft surface: case 5.

beam ion densities, neutral densities, and potentials. The parameters are given in Table 5.

We first evaluate the backflow characteristics from the parameters given in case 5. Figure 8 shows vector plots of the beam ions emitted from the FEEP emitter on an x–z plane and on a y–z plane across the center of the slit. Figure 9 shows the electric field vectors on an x–z plane across the center of the slit and two x–y planes at two different z locations away from the thruster's exit. Figures 10 and 11 show charge exchange ion vectors and phase plots respectively. Figure 12 shows the beam ion density, neutral density, and charge-exchange ion density on an x–z plane across the center of the slit.

In the region immediately outside the FEEP emitter's exit, the electric field is dominated by the negative accelerator potential and the field lines are directed toward the accelerator (Fig. 9). Most slow charge-exchange ions are generated immediately outside the FEEP emitter's exit, where both ion and neutral density are at their maximum (Fig. 12) and backflow directly to the accelerator (Fig. 10). Their density is more than three orders of magnitude below the beam ion density (Fig. 12). Few charge-exchange ions will leave this accelerator-dominated area, as indicated by the phase plot in Fig. 11. When starting at a distance of about 3 cm from the FEEP emitter's exit, ion space charge effects become more dominant, and a positive potential hump develops in the center of the beam. As the electric field develops a larger component in the direction perpendicular to the thrust direction, the ions emitted from the FEEP emitter form a divergent beam and charge exchange ions generated farther away from the FEEP emitter are pushed out of the plume with an initial velocity transverse to the beam direction. Once outside of the beam region, the charge exchange ions fall under the electric field of the spacecraft and can backflow to contaminate the spacecraft surface. Here, we take that the spacecraft surface has a potential of 0 V as a boundary condition. The backflow current is so small (order of microampheres) that we neglect charging effects on the spacecraft surface (the influence would be in the order of microvolts as calculated in Ref. 15). Hence, the charge-exchange ions will only backflow toward the spacecraft surface due to the influence of the accelerator's potential.

We calculate the backflow current by integrating the number of test particles collected by the spacecraft. The total backflow current for this case is $I_B = 0.93\ \mu$A, or 0.02% of the emitter current, compared to the charge-exchange ion current lost in the simulation domain and thus escaping the accelerator potential $I_{B,\text{loss}} = 8.51$ nA. Hence, nearly all charge-exchange ion flow back to the surface. The distribution of backflow deposit on the spacecraft surface is shown in Fig. 13 in terms of monolayer. One monolayer corresponds to 10^{19} particles/m^2. Not surprisingly, the distribution of monolayers is concentrated at the accelerator, due to the negative accelerator voltage. The location of the valley corresponds to the location of the highly positive emitter, which repels the backflowing slow ions. At the maximum concentration, the backflow deposit is 3.5×10^{-3} monolayers/s. The region outside the accelerator receives a homogenous backflow deposit of 7×10^{-7} monolayers/s, about four orders of magnitude less than that received by the accelerator. This reduces the contamination risk to other parts of the spacecraft considerably.

We next change the operating conditions according to the observed current-voltage characteristics[1] (case 1–4). The calculated backflow current is listed in Table 5. Because both the ion current I_i and the emitter potential U_E are decreased, whereas the accelerator potential U_{acc} remains constant, the backflow current also decreases as expected. The backflow current calculated for case 1 is $I_B = 0.04\ \mu$A, more than one order of magnitude less than that in case 5. Figure 14 shows the distribution of backflow ion deposit on the spacecraft surface. The distribution is similar to that shown in Fig. 13. In this case, the backflow ion deposit is 2×10^{-4} monolayers/s at the location of the maximum distribution. Outside the accelerator, the backflow ion deposit is also four orders of magnitude less than the maximum value.

Simple Expression for Backflow Current Calculation

The three-dimensional particle simulations performed in the last two sections are computationally expensive. For engineering applications, it would be desirable to derive a simple, approximate scaling expression that can be used for a quick estimation of FEEP charge-exchange ion backflow. Here, we derive such scaling based on simulation results.

The total charge exchange ion current is given by $I_{\text{CEX}} = -e \cdot \mathrm{d}N_{\text{CEX}} \cdot V_{\text{CEX}}/\mathrm{d}t$ where V_{CEX} is the volume of charge-exchange ion production. Only part of it will be collected as a backflow current, depending on the accelerator specifications. The charge-exchange ion production is dominated by that in the proximity of the emitter slit where both the beam ion and neutral density are at their maximum. Hence, the total backflow current is then approximately given by

$$I_B = \frac{\mathrm{d}N_{\text{CEX}} \cdot V_{\text{CEX}}}{\mathrm{d}t} \cdot e = V_{\text{CEX}} \cdot \frac{I_i^2 \cdot \gamma \cdot (100-\gamma)}{e \cdot A_i \cdot A_n \cdot v_n \cdot 100} \cdot \sigma_{\text{CEX}}(v_i)$$

$$\approx C(A_{\text{acc}}, U_{\text{acc}}) \cdot I_i^2 \cdot \gamma \cdot \frac{(100-\gamma)}{100} \cdot \left[k_1 \cdot \ell n \left(\sqrt{\frac{2 \cdot e \cdot U_E - U_{\text{acc}}}{m_i}} \right) + k_2 \right]^2 \tag{16}$$

where C is a proportional constant depending on the accelerator area A_{acc} and the accelerator potential U_{acc}, which together with space charge effects define the emitter exit potential.

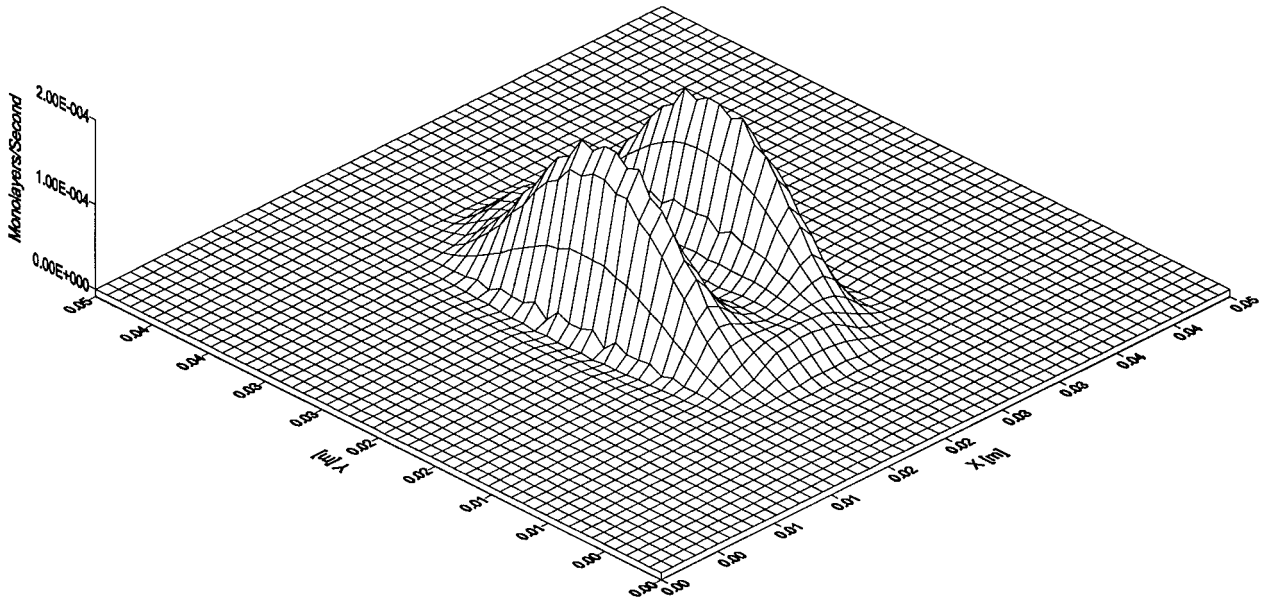

Fig. 14 Distribution of monolayers/s on the spacecraft surface: case 1.

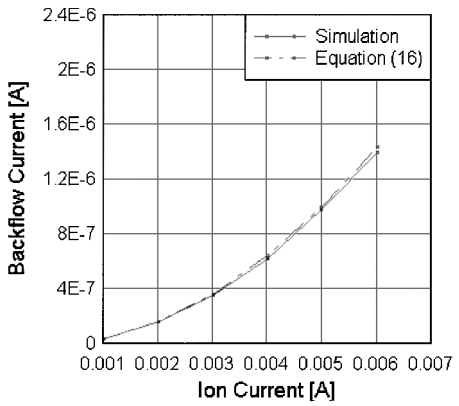

Fig. 15 Comparison of simulation and approximation from cases 1 and 6 (ion current variation).

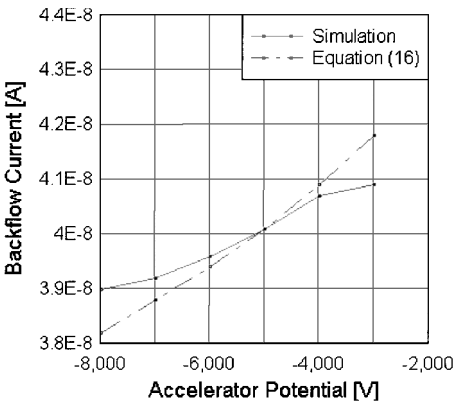

Fig. 17 Comparison of simulation and approximation from cases 1 and 8 (accelerator potential variation).

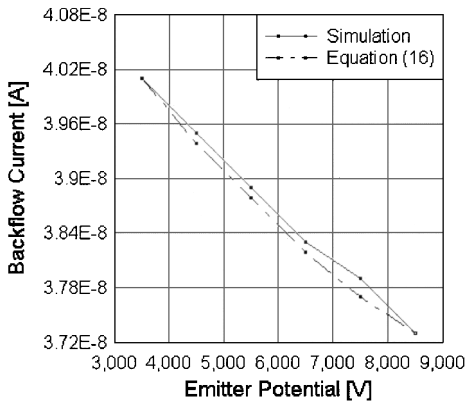

Fig. 16 Comparison of simulation and approximation from cases 1 and 7 (emitter potential variation).

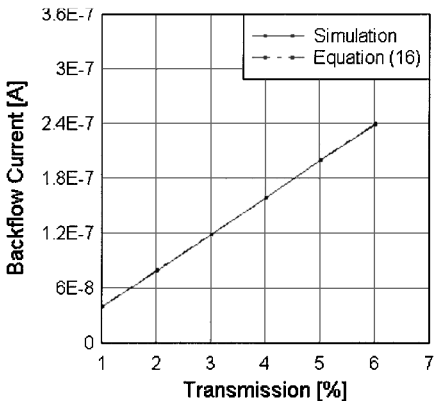

Fig. 18 Comparison of simulation and approximation from cases 1 and 9 (transmission factor variation).

In cases 6–9 from Table 5, we vary one parameter per simulation set (ion current, emitter potential, accelerator potential, transmission factor) and plot the simulation data against the approximation given by Eq. (16), shown in Figs. 15–18. Different emitter and accelerator designs require another evaluation for a new set of correction and proportional factors. The correction factor C was determined from a curve fit as $C = 4.3 \times 10^{16}$ sm^{-2}C^{-1}. For very quick estimations, the order of magnitude can be determined from $C \approx e \cdot v_n^{-1}$, which in these cases leads to 2.83×10^{16} sm^{-2}C^{-1}. In all plots, Eq. (16) corresponds very well to the data obtained from simulation. Only the variation of the accelerator potential shows a deviation due to the strong influence on the volume V_{CEX}, which was assumed constant in Eq. (16). The maximum deviation is 2%, which is still acceptable. Our final comparison with the current-voltage characteristic from cases 1–5 is shown in Fig. 19. The agreement between approximation and simulation is very good.

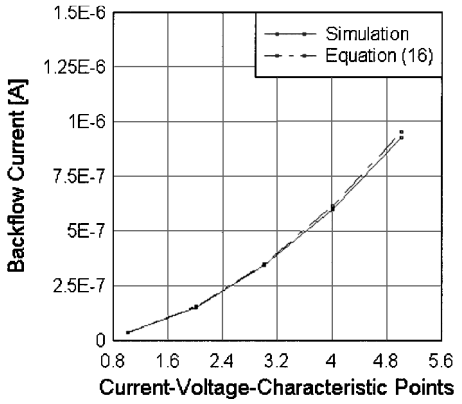

Fig. 19 Comparison of simulation and approximation from case 1 to case 5 (points along the current-voltage characteristic).

Conclusions

We have developed a three-dimensional numerical model based on full particle PIC with Monte Carlo collisions to study the induced environment from a FEEP emitter in an ambient plasma environment. The simulation model follows the propellant ions and neutral particles emitted from a FEEP emitter and electrons emitted from a thermionic neutralizer, as well as charge-exchange ions generated in the plume. Comparisons between simulations and electrostatic wire measurements show very good agreement. This model is used to evaluate charge-exchange ion backflow contamination on the spacecraft surface under different operating conditions and to investigate the effects of beam neutralization on the backflow. For engineering applications, a simple, semi-analytical expression is also derived using simulation results for a quick estimation of the backflow current.

Simulations show that the backflow charge-exchange ion current is in the order of about 0.01% of the current emission. Nearly all backflow ions are concentrated on the accelerator electrode because it has a high negative potential with respect to the spacecraft surface. The backflow current increases with the increase of emission current. To significantly reduce the backflow contamination, more efficient FEEP emitters with significantly less neutral flux emissions need to be developed.

Acknowledgments

M. Tajmar thanks the International Space University, which provided the funding for his stay at the Jet Propulsion Laboratory (JPL) during this research. This work was carried out jointly at the Vienna University of Technology and at the JPL, California Institute of Technology. We acknowledge many helpful discussions with J. Mitterauer, J. Blandino, and J. Polk.

References

[1]Mitterauer, J., "Field Emission Electric Propulsion: Mass and Optical Spectroscopy of Beam Components," Final Rept., European Space Research and Technology Centre Contract 6545/85/NL/PH, Vienna Univ. of Technology, Vienna, Oct. 1989.

[2]Mitterauer, J., "Field Emission Electric Propulsion Spectroscopic Investigations on Slit Emitters," Final Rept., European Space Research and Technology Centre Contract 5051/82/NL/PB (SC), Vienna Univ. of Technology, Vienna, Dec. 1985.

[3]Carruth, M. (ed.), "Experimental and Analytical Evaluation of Ion Thruster/Spacecraft Interactions," Jet Propulsion Lab., JPL Publication 80-92, California Inst. of Technology, Pasadena, CA, 1981.

[4]Samanta Roy, R. I., Hastings, D. E., and Gatsonis, N. A., "Numerical Study of Spacecraft Contamination and Interactions by Ion-Thruster Effluents," *Journal of Spacecraft and Rockets*, Vol. 33, No. 4, 1996, pp. 535–542.

[5]Wang, J., Brinza, D. E., Young, D. T., Nordholt, J. E., Polk, J. E., Henry, M. D., Goldstein, R., Hanley, J. J., Lawrence, D. J., and Shappirio, M., "Deep Space One Investigations of Ion Propulsion Plasma Environment," *Journal of Spacecraft and Rockets*, Vol. 37, No. 5, 2000, pp. 545–555.

[6]Marcuccio, S., Genovese, A., and Andrenucci, M., "Experimental Performance of Field Emission Microthrusters," *Journal of Propulsion and Power*, Vol. 14, No. 5, 1998, pp. 774–781.

[7]Tajmar, M., and Wang, J., "Three-Dimensional Numerical Simulation of Field-Emission-Electric-Propulsion Neutralization," *Journal of Propulsion and Power*, Vol. 16, No. 3, 2000, pp. 536–544.

[8]Andrenucci, M., Marcuccio, S., Genovese, A., "FEEP Thruster Plume Investigation with Langmuir Probes," International Electric Propulsion Conf., Rept. IEPC-95-98, Sept. 1995.

[9]Tajmar, M., Mitterauer, J., and Wang, J., "Field-Emission-Electric-Propulsion (FEEP) Plasma Modeling: Three-Dimensional Full Particle Simulations," AIAA Paper 99-2298, June 1999.

[10]Thompson, S. P., "Neutral Emissions from Liquid Metal Ion Sources," *Vacuum*, Vol. 34, No. 1–2, 1984, pp. 223–228.

[11]Rapp, D., and Francis, W. E., "Charge Exchange Between Gaseous Ions and Atoms," *Journal of Chemical Physics*, Vol. 37, No. 11, 1962, pp. 2631–2645.

[12]Birdsall, C. K., and Langdon, A. B., *Plasma Physics via Computer Simulation*, Adam Hilger, New York, 1991.

[13]Birdsall, C. K., "Particle-in-Cell Charged-Particle Simulations, Plus Monte Carlo Collisions with Neutral Atoms, PIC-MCC," *IEEE Transactions on Plasma Science*, Vol. 19, No. 2, 1991, pp. 65–85.

[14]Andrenucci, M., Ciucci, A., and Marcuccio, S., "Numerical Model of Cesium Ion Beams in Field Emission Electric Propulsion Thrusters," *Journal of Propulsion and Power*, Vol. 14, No. 6, 1998, pp. 1027–1035

[15]Tajmar, M., Gonzales, J., and Hilgers, A., "Modeling of Spacecraft-Environment Interactions on SMART-1," *Journal of Spacecraft and Rockets* (submitted for publication).

I. D. Boyd
Associate Editor